Optical Chopper Driven by the Casimir Force

G. L. Klimchitskaya,[1,2,*] V. M. Mostepanenko,[1,2,3] V. M. Petrov,[4] and T. Tschudi[5]

[1] *Central Astronomical Observatory at Pulkovo of the Russian Academy of Sciences, Saint Petersburg 196140, Russia*

[2] *Institute of Physics, Nanotechnology and Telecommunications, Peter the Great Saint Petersburg Polytechnic University, Saint Petersburg 195251, Russia*

[3] *Kazan Federal University, Kazan 420008, Russia*

[4] *Institute of Advanced Manufactoring Technologies, Peter the Great Saint Petersburg Polytechnic University, Saint Petersburg 195251, Russia*

[5] *Institute of Applied Physics, Darmstadt University of Technology, Hochschulstrasse 6, Darmstadt 64289, Germany*

(Received 28 December 2017; revised manuscript received 7 March 2018; published 13 July 2018)

We propose an experimental scheme and present detailed theoretical description of the optical chopper in which functionality is based on the balance between the Casimir and light pressures. The proposed device consists of two atomically thin metallic mirrors forming the Fabry-Perot microfilter. One of the mirrors is deposited on a solid cube and another on a thinner wall subjected to bending under the influence of attractive Casimir force and repulsive force due to the pressure of light from a continuous laser amplified in the resonator of a microfilter. The separation distance between the mirrors should only slightly exceed the half wavelength of the laser light. It is shown that in this case the resonance condition in the microfilter alternatively obeys and breaks down resulting in the periodic pulses of the transmitted light. The Casimir pressure is calculated taking into account an anisotropy of the dielectric permittivity of a metal at several first Matsubara frequencies. The reflectivity properties of atomically thin metallic mirrors in the optical spectral range are found using the experimentally consistent phenomenological approach developed earlier in the literature. The specific values of all parameters, found for the microfilter made of quartz glass with Ag mirrors, demonstrate its workability. The proposed optical chopper may find prospective applications in the emerging field of nanotechnology exploiting the effects of quantum fluctuations.

DOI: 10.1103/PhysRevApplied.10.014010

I. INTRODUCTION

In the last few decades, advances in the integrated-circuit fabrication techniques allowed the production of microelectomechanical (MEMS) and nanoelectromechanical (NEMS) systems with sizes ranging from micrometers to nanometers [1]. It is common knowledge that MEMS and NEMS devices are increasingly used in optical and cellular communications, as well as in a variety of sensors and in many other applications. As observed more than 30 years ago [2,3], upon shrinking MEMS dimensions to submicrometer level, in addition to electric forces, the van der Waals [4] and Casimir [5] forces induced by the electromagnetic fluctuations come into play. These forces act between uncharged material surfaces and become dominant at separations of several nanometers and several hundred nanometers, respectively. In an early stage, the combined action of the Casimir and elastic forces in MEMS devices has been studied in Ref. [6]. Later on the role of roughness and electrostatic effects was also considered in Refs. [7,8].

Experimentally, the combined role of the electrostatic and Casimir forces in the loss of MEMS device functionality, when the moving part of it jumps to a fixed electrode, was investigated in Refs. [9,10]. This phenomenon is called a *pull-in* or *stiction*. A short time later it was experimentally demonstrated that the Casimir force is not only detrimental to MEMS and NEMS functionality, but can also be used for actuation of microdevices in place of the electric force [11,12]. The original device created in Refs. [11,12] has been called a *micromechanical Casimir oscillator*. In the next few years, this device was refined and actively exploited for both precise measurements of the Casimir interaction in fundamental physics and for creation of novel MEMS and NEMS (see Refs. [13,14] for a review).

In recent years, a considerable number of high-precision experiments on measuring the Casimir interaction between smooth surfaces of metallic [15–23] and semiconductor [24–34] test bodies have been performed by means of an

*g_klimchitskaya@mail.ru

atomic force microscope and a micromechanical oscillator. In several Casimir experiments, the structured (sinusoidally and rectangular corrugated) test bodies have also been used [35–39]. All of this gave impetus to diverse applications of the obtained results to MEMS and NEMS devices driven by the Casimir force. Thus, the role of the geometry and dielectric properties of materials in the stability of Casimir-force-actuated nanodevices was analyzed in Refs. [40,41]. The actuation of MEMS under the influence of Casimir force with account of surface roughness and amorphous to crystalline phase transformations was investigated [42–44]. Casimir forces on a silicon micromechanical chip have been experimentally demonstrated in Refs. [45,46]. In Ref. [47], the method of how to control the mechanical switch was suggested using an enhancement of the Casimir force between a graphene sheet and a silicon membrane. We note, however, that the scheme of the Casimir switch suggested in Ref. [48], as a possibility to significantly alter the optical-output rate by the vacuum force, is inoperative. As the authors themselves recognize, measurements of the Casimir force in the separation region from 0.7 to 2 nm, required in their scheme, are challenging. Of even greater concern is the fact that Ref. [48] uses an ideal-metal expression for the Casimir force between gold-coated surfaces at so short separations and, thus, overestimates the force magnitude by at least a factor of 20 [49].

In this paper, we propose the possibility of creating the optical chopper driven by the Casimir force. The feasibility of our proposal is supported with detailed theory. The key element of the proposed setup is the SiO_2 microdevice incorporating the Fabry-Perot microfilter with two parallel thin metallic mirrors which form a microresonator. The left mirror should be deposited on the side of a solid SiO_2 cube and the right one on a relatively thin SiO_2 wall subjected to bending under the influence of the Casimir force acting between the two mirrors in high vacuum. Note that detection of the mechanical deformation of a macroscopic object induced by the Casimir force was made in Refs. [50,51] by means of an adaptive holographic interferometer. The length of a resonator cavity (i.e., the separation distance between the foot parts of the mirrors) should be made only slightly larger than the half wavelength $\lambda/2$ of the laser light incident from the left. In the absence of laser light, the Casimir force shifts the top of the right mirror slightly closer to the top of the left one than their foot parts. This is a stable position where the Casimir force is balanced by the restoring elastic force. As a result, when the laser is switched on and the light beam enters a microfilter through the SiO_2 cube and the left mirror, the effective resonator length at the beam section will be approximately equal to $\lambda/2$. This leads to a cyclic process. First, the amplitude of a standing wave in the filter resonator will instantaneously increase, resulting in detection of a relatively high level of transmitted light intensity. The repulsive force due to the light pressure in the resonator will compensate the Casimir force and the right mirror will become vertical. This is an unstable position where the elastic force vanishes. The effective resonator length here is larger than $\lambda/2$, violating the resonance condition. Then, the wave amplitude in the gap will fall down, leading to transmitted light intensity of almost zero level. Finally, the Casimir force, which will not be balanced by the repulsive force due to light pressure any more, will return the right mirror to its initial position where the wall is slightly tilted to the left. Here, the resonance condition for the incident light beam is again obeyed with sufficient precision, and the next cycle starts.

We emphasize that the proposed microresonator should not be considered as an optomechanical cavity, which usually consists of a fixed mirror and mechanical oscillator, i.e., another mirror is attached to a spring (see the monograph [52] and review [53]). The point is that, for optomechanical cavities, the dynamics of the second mirror is important for the functionality of a device. This is, however, not the case for the proposed optical chopper which is driven not by a mechanical force or a mechanical force in combination with the light pressure, but mostly by the Casimir force acting on the right mirror deposited on a wall. This is reached due to the chosen initial position of the foot part of the right mirror at more than $\lambda/2$ separation from the left one, i.e., at a distance where the resonance condition is violated. In this case, one does not need to know a detailed dynamics of the system to prove the existence of the cyclic process (see Secs. II and IV for more details, including the role of optomechanical effects).

We develop a theoretical description of the physical processes in the experimental setup described above. The Casimir force is calculated on the basis of the Lifshitz theory at nonzero temperature with account of an anisotropy of the dielectric permittivities for thin metallic films, forming the resonator mirrors, at several first Matsubara frequencies [54]. The reflectance and transmittance of mirrors forming the Fabry-Perot filter at the used laser wavelength are found with due regard to increased transparency of atomically thin metallic films [55]. The light pressure in the resonator is also calculated. The balance between calculated Casimir and light pressures enables one to predict the formation of pulses in the transmitted light. We argue that the designed device is advantageous as compared to the commonly used mechanical optical choppers exploiting the wheels of various shape, which should have a highly stable rotating speed.

The paper is organized as follows. In Sec. II, we present some details of the proposed setup. Section III contains calculations of the Casimir pressure in the experimental configuration. In Sec. IV, we find the force due to the light pressure and its balance with the Casimir force. In Sec. V, the reader will find our conclusions and a discussion.

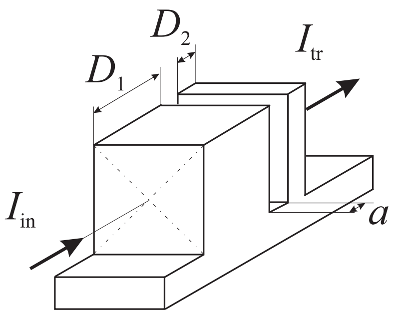

FIG. 1. Schematic of the SiO_2 microdevice incorporating the Fabry-Perot microfilter with length a (see text for further discussion).

II. PROPOSED SETUP

The heart of the proposed optical chopper driven by the Casimir force is a SiO_2 microdevice, which can be manufactured using the technique of ion-beam etching. The main part of this device is the Fabry-Perot microfilter formed by a cube with the side $D_1 = 50$ μm and a square wall of thickness $D_2 = 5$ μm of the same side length. Both the cube and the wall are located at the joint base parallel to each other (see Fig. 1). The right face of the cube and the left face of the wall in Fig. 1 should be coated by thin metallic layers to form the resonator mirrors of the filter. The thickness of the mirrors d could be in the range from 0.5 to 3 nm. The resonator length (i.e., the distance between metallic mirrors) is notated a.

Some details on how to fabricate microdevices, like the one shown in Fig. 1, can be found in the literature on measurements of the Casimir force and its applications in nanotechnology. Although fabrication of large-area microstructures with a uniform gap width of several hundred nanometers and vertical sidewalls remains challenging [39], the nanofabrication processes are developed to allow the production of two interacting surfaces that are automatically aligned and almost parallel to each other [39,45]. In so doing, with the etch mask defined by electron-beam lithography, a high degree of parallelism is ensured [45]. The deposition of metallic mirrors can be performed by either electroplating or sputtering [39]. Another technology of producing a microdevice shown in Fig. 1 suggests manufacturing the two halves of this device separately. Then both halves should be placed into a vacuum chamber where the metallic mirrors are deposited. The assembly and alignment of the entire device should be made inside the vacuum chamber using the high-precision positioning technology described in Refs. [50,51,56].

As a source of light of intensity I_{in} incident on the SiO_2 microdevice in the proposed experiment, a cw Nd:YAG laser with a wavelength of the second harmonic $\lambda = 532.0$ nm can be used. It is suggested to fabricate the resonator with length equal to $a = \lambda/2 + \Delta\lambda$, where $\Delta\lambda$ is sufficiently large to break down the resonance condition

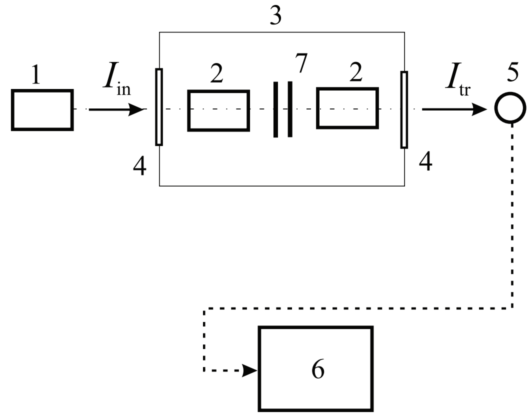

FIG. 2. General scheme of the optical chopper driven by the Casimir force: 1, laser; 2, beam-forming systems; 3, vacuum chamber; 4, optical windows; 5, photodetector; 6, two-channel oscilloscope; 7, Fabry-Perot microfilter.

$a \approx \lambda/2$ in the absence of any external force. For smaller a, i.e., for $|a - \lambda/2| < \Delta\lambda$, the resonance condition is assumed to be obeyed with sufficient precision (see Sec. IV for the specific values of $\Delta\lambda$).

The SiO_2 system should incorporate two pairs of the optical windows and beam-forming systems inserted into the vacuum chamber (see Fig. 2) at sufficiently low pressure of about $10^{-6} - 10^{-7}$ Torr. Beam-forming systems are needed to form the light beams having Gaussian-like profiles with the diameter equal to approximately 40 μm for the wavelength of 532.0 nm. The transmitted light beam can be detected by a photodetector (see Fig. 2). Special attention should be paid to the stability of the setup. For this purpose, it is desirable to deposit the vacuum chamber on the optical table with an active air-pumped stabilization.

It is expected that the photodetector will register pulses of light transmitted through the Fabry-Perot microfilter, i.e., the high level of transmitted light intensity will alternate with periods when the intensity of transmitted light reduces to almost zero. According to Sec. I, this expectation is based on the action of the Casimir force. When the laser is switched off, this force slightly tilts the wall of our microdevice in the direction of the left mirror. As a result, the separation distance between the mirrors decreases and the resonance condition $a \approx \lambda/2$ is obeyed with sufficient precision. In this initial position, the Casimir force is balanced by the restoring elastic force. After the laser is switched on, the amplitude of the standing wave in the gap between the mirrors will instantaneously increase, taking into account a rather high-quality factor of the resonator (see Sec. IV). Because of this, the photodetector will detect a high level of transmitted light, and the repulsive force due to the light pressure in the gap will compensate the attractive Casimir force. Thus, the wall will take the vertical position where it is separated from the left mirror by the distance $a = \lambda/2 + \Delta\lambda$. In this position, the elastic force is equal to zero but the resonance condition breaks down, leading to an instantaneous drop of the wave amplitude in the gap and to a low level of transmitted light intensity. At this stage, the attractive Casimir force returns the wall to its initial (tilted) position, where it is balanced by the elastic force. In this position, the resonance condition $a \approx \lambda/2$ is again obeyed with sufficient precision, and the next cycle starts.

In Secs. III and IV, these qualitative considerations receive quantitative confirmation by using the Lifshitz theory of the Casimir force and calculating the parameters of a microfilter. As already noted in Sec. I, the proposed microresonator should not be considered as an optomechanical cavity which incorporates a mechanical oscillator and gives rise to the process of light-induced cyclic response, i.e., self-excited oscillation. This is already seen from the fact that, in the absence of the Casimir force, no oscillation arises in our microresonator with the laser light on (because in this case the right mirror would be vertical and the resonance condition is, thus, violated). In the proposed setup, it is only the Casimir force which leads to a fulfilment of the resonance condition in the initial position of a cycle by tilting the wall to the left in the absence of laser light, and it is the light pressure which leads to a violation of this condition when the wall becomes vertical. Thus, if it is possible to ensure the balance between the Casimir and light pressures (see Sec. IV), the suggested configuration clearly undergoes a cyclic process even if the details of an intermediate dynamics remain unknown. Note also that the dynamics of an optomechanical cavity formed by a stationary mirror made of dielectric Si and an oscillating Al mirror was considered in Ref. [57] with account of the Casimir force and Coulomb interaction due to trapped charges, and a partial agreement between experiment and theory was reached.

III. CALCULATION OF THE CASIMIR PRESSURE

We start by calculating the Casimir pressure in the configuration of a microdevice described in Sec. II. It consists of a SiO_2 cube with the side $D_1 = 50$ μm, whose right face is coated by the metallic film of thickness d, and parallel to it the SiO_2 wall of the same area. The thickness of this wall is $D_2 = 5$ μm. The left face of the wall is also coated by metallic film of thickness d. The separation distance between the cube and the wall is only slightly larger than $\lambda/2 = 266$ nm (compare Figs. 3 and 1). Taking into account that $D_1 \gg a$, one can consider the opposite faces of a cube and a wall as having an infinitely large area. However, the finite thickness of the cube, of the wall, and of the metallic coatings should be taken into account in computations of the Casimir pressure. In so doing, we also take proper account of the anisotropy of atomically thin metallic films of thickness d, which are described as uniaxial crystals [54].

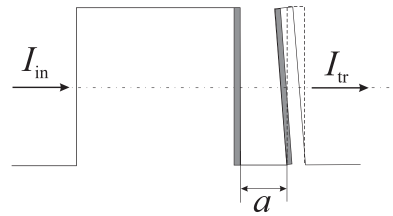

FIG. 3. Configuration of the resonator in the Fabry-Perot microfilter. Metallic mirrors are not shown to scale and are indicated by dark gray.

The microdevice under consideration is assumed to be at temperature T in thermal equilibrium with the environment. In this case, the Casimir pressure acting on the wall is given by the following Lifshitz formula for the four-layer system [5,49,58,59]:

$$P(a,T) = -\frac{k_BT}{\pi}\sum_{l=0}^{\infty}{}' \int_0^\infty k_\perp dk_\perp q_l \times \left\{\left[\frac{e^{2aq_l}}{R_{\mathrm{TM},l}^{(1)}R_{\mathrm{TM},l}^{(2)}} - 1\right]^{-1} + \left[\frac{e^{2aq_l}}{R_{\mathrm{TE},l}^{(1)}R_{\mathrm{TE},l}^{(2)}} - 1\right]^{-1}\right\}. \quad (1)$$

Here, k_B is the Boltzmann constant, the prime on the summation sign multiplies the term with $l = 0$ by $1/2$, $k_\perp = |\boldsymbol{k}_\perp|$ is the magnitude of the projection of the wave vector on the plane of the wall, and the factor q_l is defined as

$$q_l = \sqrt{k_\perp^2 + \frac{\xi_l^2}{c^2}}, \quad (2)$$

where $\xi_l = 2\pi k_BTl/\hbar$ with $l = 0, 1, 2, \ldots$ are the Matsubara frequencies.

The amplitude reflection coefficients $R_{\mathrm{TM(TE)},l}^{(i)}$ on the left ($i = 1$) and right ($i = 2$) plates of our device at the Matsubara frequencies entering the Lifshitz formula (1) are defined for two independent polarizations of the electromagnetic field, transverse magnetic (TM), and transverse electric (TE), and have the form [5,49,58,59]

$$R_{\mathrm{TM(TE)},l}^{(i)} \equiv R_{\mathrm{TM(TE)}}^{(i)}(i\xi_l, k_\perp) = \frac{r_{\mathrm{TM(TE)},l}^{(v,m)} + R_{\mathrm{TM(TE)},l}^{(g,i)}\, e^{-2dk_{\mathrm{TM(TE)},l}^{(m)}}}{1 + r_{\mathrm{TM(TE)},l}^{(v,m)} R_{\mathrm{TM(TE)},l}^{(g,i)}\, e^{-2dk_{\mathrm{TM(TE)},l}^{(m)}}}. \quad (3)$$

In this equation, the quantities $k^{(m)}_{\mathrm{TM(TE)},l}$, related to anisotropic metallic films, are given by [5,60,61]

$$k^{(m)}_{\mathrm{TM},l} \equiv k^{(m)}_{\mathrm{TM}}(i\xi_l, k_\perp) = \sqrt{\frac{\varepsilon^{(m)}_{xx,l}}{\varepsilon^{(m)}_{zz,l}} k_\perp^2 + \varepsilon^{(m)}_{xx,l}\frac{\xi_l^2}{c^2}},$$
$$k^{(m)}_{\mathrm{TE},l} \equiv k^{(m)}_{\mathrm{TE}}(i\xi_l, k_\perp) = \sqrt{k_\perp^2 + \varepsilon^{(m)}_{xx,l}\frac{\xi_l^2}{c^2}}, \qquad (4)$$

where the components of the diagonal dielectric tensor of a metal are $\varepsilon^{(m)}_{xx,l} \equiv \varepsilon^{(m)}_{xx}(i\xi_l) = \varepsilon^{(m)}_{yy}(i\xi_l)$, $\varepsilon^{(m)}_{zz,l} \equiv \varepsilon^{(m)}_{zz}(i\xi_l)$, and we assume that the plane (x, y) is parallel to the wall and the z axis is perpendicular to it.

Now we specify the amplitude reflection coefficients entering Eq. (3). The coefficients $r^{(v,m)}_{\mathrm{TM(TE)},l}$ describe reflections of the electromagnetic waves at the boundary plane between vacuum and a semispace made of an anisotropic metal. They take the form [5,60,61]

$$r^{(v,m)}_{\mathrm{TM},l} \equiv r^{(v,m)}_{\mathrm{TM}}(i\xi_l, k_\perp) = \frac{\varepsilon^{(m)}_{xx,l} q_l - k^{(m)}_{\mathrm{TM},l}}{\varepsilon^{(m)}_{xx,l} q_l + k^{(m)}_{\mathrm{TM},l}},$$
$$r^{(v,m)}_{\mathrm{TE},l} \equiv r^{(v,m)}_{\mathrm{TE}}(i\xi_l, k_\perp) = \frac{q_l - k^{(m)}_{\mathrm{TE},l}}{q_l + k^{(m)}_{\mathrm{TE},l}}. \qquad (5)$$

The coefficients $R^{(g,i)}_{\mathrm{TM(TE)},l}$ with $i = 1, 2$ can be presented similar to Eq. (3):

$$R^{(g,i)}_{\mathrm{TM(TE)},l} \equiv R^{(g,i)}_{\mathrm{TM(TE)}}(i\xi_l, k_\perp) = \frac{r^{(m,g)}_{\mathrm{TM(TE)},l} + r^{(g,v)}_{\mathrm{TM(TE)},l} e^{-2D_i k_l^{(g)}}}{1 + r^{(m,g)}_{\mathrm{TM(TE)},l} r^{(g,v)}_{\mathrm{TM(TE)},l} e^{-2D_i k_l^{(g)}}}, \qquad (6)$$

where

$$k_l^{(g)} \equiv k^{(g)}(i\xi_l, k_\perp) = \sqrt{k_\perp^2 + \varepsilon_l^{(g)}\frac{\xi_l^2}{c^2}}, \qquad (7)$$

and $\varepsilon_l^{(g)} \equiv \varepsilon^{(g)}(i\xi_l)$ is the dielectric permittivity of quartz glass SiO_2.

The amplitude reflection coefficients entering Eq. (6) are specified as follows. The coefficients $r^{(m,g)}_{\mathrm{TM(TE)},l}$ describe reflection at the boundary plane between the semispaces made of an anisotropic metal and a SiO_2 glass. They are given by [5,60,61]

$$r^{(m,g)}_{\mathrm{TM},l} \equiv r^{(m,g)}_{\mathrm{TM}}(i\xi_l, k_\perp) = \frac{\varepsilon_l^{(g)} k^{(m)}_{\mathrm{TM},l} - \varepsilon^{(m)}_{xx,l} k_l^{(g)}}{\varepsilon_l^{(g)} k^{(m)}_{\mathrm{TM},l} + \varepsilon^{(m)}_{xx,l} k_l^{(g)}},$$
$$r^{(m,g)}_{\mathrm{TE},l} \equiv r^{(m,g)}_{\mathrm{TE}}(i\xi_l, k_\perp) = \frac{k^{(m)}_{\mathrm{TE},l} - k_l^{(g)}}{k^{(m)}_{\mathrm{TE},l} + k_l^{(g)}}. \qquad (8)$$

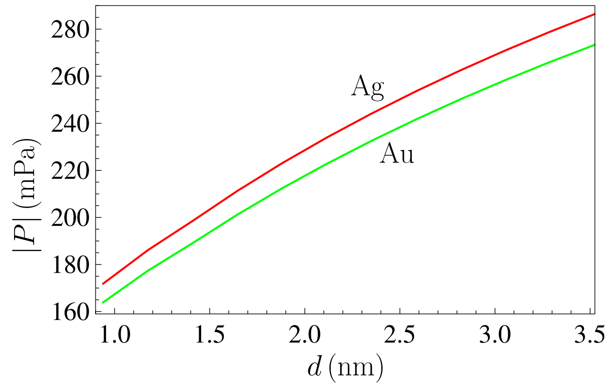

FIG. 4. Computational results for the magnitude of the Casimir pressure in the Fabry-Perot microfilter are shown by the top and bottom lines as functions of mirror thickness at the separation $a = \lambda/2$ between the mirrors made of Ag and Au, respectively.

Finally, the coefficients $r^{(g,v)}_{\mathrm{TM(TE)},l}$ at the boundary plane between a SiO_2 semispace and vacuum have the form

$$r^{(g,v)}_{\mathrm{TM},l} \equiv r^{(g,v)}_{\mathrm{TM}}(i\xi_l, k_\perp) = \frac{k_l^{(g)} - \varepsilon_l^{(g)} q_l}{k_l^{(g)} + \varepsilon_l^{(g)} q_l},$$
$$r^{(g,v)}_{\mathrm{TE},l} \equiv r^{(g,v)}_{\mathrm{TE}}(i\xi_l, k_\perp) = \frac{k_l^{(g)} - q_l}{k_l^{(g)} + q_l}. \qquad (9)$$

The dielectric permittivity of vitreous SiO_2 at the Matsubara frequencies, required for Casimir pressure computations using Eqs. (1)–(9), is taken from Ref. [62]. For the metal of resonator mirrors, we have first chosen Au most often used in precise experiments on measuring the Casimir force [13–39]. The dielectric tensor of thin Au films consisting of $n = 1$, 3, 6, and 15 atomic layers (i.e., for film thicknesses of 0.235, 0.705, 1.41, and 3.525 nm) is found in Ref. [54] within density-functional theory. It takes into account the effects of anisotropy and uses the optical data of Ref. [63] for the complex index of refraction of Au extrapolated to zero frequency by means of the Drude model. Note that for the atomically thin metallic films, the obtained results do not depend on whether the Drude or the plasma model is used for extrapolation of the data to zero frequency [60].

The computational results for the magnitude of negative (attractive) Casimir pressure are obtained at $T = 300$ K as a function of the number of atomic layers in the Au films and interpolated in the region of film thicknesses from 1 to 3.5 nm. The calculated Casimir pressures at the separation $a = \lambda/2 = 266$ nm are shown by the bottom line in Fig. 4. It turns out, however, that Au is rather disadvantageous as a material of mirrors in a microfilter due to the low reflectivity at the chosen wavelength (see Sec. IV). Because of this, the computations of the Casimir pressure are repeated for Ag mirrors. Silver has almost the same lattice parameter as Au [64]. This allows one to use the same data for $\varepsilon_{xx}^{(\mathrm{Ag})}/\varepsilon_{\mathrm{isotr}}^{(\mathrm{Ag})}$ and $\varepsilon_{zz}^{(\mathrm{Ag})}/\varepsilon_{\mathrm{isotr}}^{(\mathrm{Ag})}$, as computed in Ref. [54] for Au, and to multiply the dielectric permittivity of an isotropic (bulk) Ag, $\varepsilon_{\mathrm{isotr}}^{(\mathrm{Ag})}$, found from the tabulated optical data of Ref. [63] by these factors. The computational results for the magnitude of the Casimir pressure in the resonator with Ag mirrors are shown in Fig. 4 as a function of mirror thickness at $a = \lambda/2 = 266$ nm by the top line.

IV. BALANCE OF LIGHT AND CASIMIR PRESSURES

The intensity of light incident on the Fabry-Perot filter is I_{in} (see Figs. 1 and 3). After the integration of I_{in} over the beam area, one obtains the value of power $N_{\mathrm{in}} \approx 7$ mW for the chosen laser. Taking into account the high transparency of quartz glass at the wavelength $\lambda = 532$ nm ($\omega = 3.54 \times 10^{15}$ rad/s), one can neglect the losses in the SiO_2 cube and assume that the same power N_{in} falls on the left metallic mirror. According to Fig. 3, the mirror borders the glass cube from the left and the vacuum gap from the right. These two media can be considered as semispaces. Then, the magnitude of the amplitude reflection coefficient on the metallic film of thickness d at the normal incidence is given by [65]

$$|R| = \left| \frac{\tilde{r}^{(v,m)} + \tilde{r}^{(m,g)} e^{-2i(\omega/c)d\sqrt{\varepsilon^{(m)}}}}{1 + \tilde{r}^{(v,m)}\tilde{r}^{(m,g)} e^{-2i(\omega/c)d\sqrt{\varepsilon^{(m)}}}} \right|, \tag{10}$$

where for the complex dielectric permittivity of metal at the frequency ω we have $\sqrt{\varepsilon^{(m)}} = n^{(m)} + i\kappa^{(m)}$. For the metals used below, we have $n^{(\mathrm{Au})} = 0.543$, $\kappa^{(\mathrm{Au})} = 2.25$, and $n^{(\mathrm{Ag})} = 0.129$, $\kappa^{(\mathrm{Ag})} = 3.19$ [63]. Note that ω is sufficiently high, so that the role of anisotropy discussed in Sec. III to calculate the Casimir pressure determined by much lower frequencies is negligibly small. Because of this, the reflection coefficients $\tilde{r}^{(v,m)}$ and $\tilde{r}^{(m,g)}$ are given by Eqs. (5) and (8) where one should put $\varepsilon_{xx}^{(m)} = \varepsilon_{zz}^{(m)}$ and replace $i\xi_l$ with ω (we recall that at the normal incidence $k_\perp = 0$, and the TM and TE reflection coefficients coincide).

In fact, Eq. (10) is applicable for sufficiently thick films. As mentioned in Sec. I, atomically thin metallic films are characterized by the increased transparency and this fact should be taken into account in computations. There are several phenomenological approaches developed to gain a better understanding of relevant physical mechanisms (see, e.g., [55,66–70]). According to the approach of Refs. [68–70], for atomically thin metallic films illuminated with visible light at the normal incidence, good agreement with the measurement results is reached if in the coefficients $\tilde{r}^{(v,m)}$ and $\tilde{r}^{(m,g)}$ entering Eq. (10) one puts $\kappa^{(m)} = 0$. In this case we obtain

$$\tilde{r}^{(v,m)} = \frac{n^{(m)} - 1}{n^{(m)} + 1}, \quad \tilde{r}^{(m,g)} = \frac{n^{(g)} - n^{(m)}}{n^{(g)} + n^{(m)}}, \tag{11}$$

where $n^{(g)} = \sqrt{\varepsilon^{(g)}} \approx 1.46$ is the real refractive index of SiO_2 at the used frequency $\omega = 3.54 \times 10^{15}$ rad/s.

Substituting Eq. (11) in Eq. (10), for the reflectance of metallic film $\mathcal{R} = |R|^2$ at the frequency ω one finds

$$\mathcal{R} = \frac{\tilde{r}^{(v,m)2} + \tilde{r}^{(m,g)2} e^{-2\alpha d} - 2\tilde{r}^{(v,m)}\tilde{r}^{(m,g)} e^{-\alpha d}\cos\psi}{1 + \tilde{r}^{(v,m)2}\tilde{r}^{(m,g)2} e^{-2\alpha d} - 2\tilde{r}^{(v,m)}\tilde{r}^{(m,g)} e^{-\alpha d}\cos\psi}, \tag{12}$$

where

$$\alpha = \frac{4\pi\kappa^{(m)}}{\lambda}, \quad \psi = \frac{4\pi n^{(m)} d}{\lambda}. \tag{13}$$

In a similar way, for the transmittance of our film we have

$$\mathcal{T} = \frac{\tilde{t}^{(v,m)}\tilde{t}^{(m,g)} e^{-\alpha d}}{1 + \tilde{r}^{(v,m)2}\tilde{r}^{(m,g)2} e^{-2\alpha d} - 2\tilde{r}^{(v,m)}\tilde{r}^{(m,g)} e^{-\alpha d}\cos\psi}, \tag{14}$$

where the respective coefficients are given by

$$\tilde{t}^{(v,m)} = \frac{4n^{(m)}}{(1 + n^{(m)})^2}, \quad \tilde{t}^{(m,g)} = \frac{4n^{(m)} n^{(g)}}{(n^{(m)} + n^{(g)})^2}. \tag{15}$$

As a result, for the absorptance of light by an atomically thin metallic film of thickness d we obtain

$$\mathcal{A} = 1 - \mathcal{R} - T. \tag{16}$$

According to Sec. III, the most often used metal in Casimir physics is Au [5,13]. However, the rather low reflectivity of Au in the visible light makes it unsuitable for use in the Fabry-Perot filter. Thus, even at the boundary plane between an Au semispace and vacuum $\mathcal{R}_{\mathrm{ss}}^{(\mathrm{Au})} = 0.71$. For the atomically thin films used below (d varies from 0.94 to 1.41 nm) the reflectance $\mathcal{R}^{(\mathrm{Au})}$ computed using Eq. (12) varies from approximately 0.36 to 0.32, i.e., is even much lower.

Because of this, we choose Ag as the metal of the mirrors in the proposed setup. In this case, Eq. (12) leads to $\mathcal{R}^{(\mathrm{Ag})} = 0.938$ for the film of $d = 0.94$ nm thickness and to $\mathcal{R}^{(\mathrm{Ag})} = 0.930$ for the film with $d = 1.41$ nm. The respective values of the film transmittance $\mathcal{T}^{(\mathrm{Ag})}$ computed using Eq. (14) are 0.044 and 0.043. In this case, the values of the absorptance of light by one mirror $\mathcal{A}^{(\mathrm{Ag})}$ computed by Eq. (16) are equal to 0.018 and 0.027, respectively.

Assuming that for both mirrors the values of $\mathcal{R}^{(\mathrm{Ag})}$ and $\mathcal{T}^{(\mathrm{Ag})}$ are equal and that the power of light entering the resonator is amplified by the factor of q, one finds for the transmission coefficient [71]

$$\tau = \left(1 - \frac{\mathcal{A}^{(\mathrm{Ag})}}{1 - \mathcal{R}^{(\mathrm{Ag})}}\right)^2, \tag{17}$$

where $q = 1/(1 - \mathcal{R}^{(\mathrm{Ag})})^2$ represents the quality factor in our formalism. The coefficient τ allows calculation of the power of light transmitted through the resonator $N_{\rm tr} = \tau N_{\rm in}$. For the two microresonators with mirror thicknesses equal to 0.94 and 1.41 nm, we obtain from Eq. (17) $\tau = 0.50$ and 0.38, respectively, i.e., $N_{\rm tr} = 3.5$ and 2.66 mW. This means that for the two microresonators under consideration the light power passed through the left mirror (it is equal to $N_{\rm in}\mathcal{T}^{(\rm Ag)} = 0.31$ and 0.30 mW) is amplified by factors of 260 and 206, respectively.

Now we are in a position to determine the thickness of resonator mirrors furnishing a balance between the Casimir and light pressures. The pressure of light amplified in the resonator is given by [71]

$$P_{\rm light} = \frac{1}{c}(1 + \mathcal{R}^{(\rm Ag)})I_{\rm res}, \tag{18}$$

where the amplified intensity is $I_{\rm res} = qI_{\rm in}\mathcal{T}^{(\rm Ag)}$. Then the condition that the Casimir force acting on a SiO_2 wall is compensated by the force due to the light pressure takes the form

$$\int_S P_{\rm light}dS \approx \left|P\left(\frac{\lambda}{2} + \Delta\lambda\right)\right| D_1^2, \tag{19}$$

where the integration is performed over the area of the light beam.

Substituting Eq. (18) in Eq. (19), one obtains

$$\frac{1}{c}(1 + \mathcal{R}^{(\rm Ag)})N_{\rm res} \approx \left|P\left(\frac{\lambda}{2} + \Delta\lambda\right)\right| D_1^2, \tag{20}$$

where the power of light, amplified in the resonator, is $N_{\rm res} = qN_{\rm in}\mathcal{T}^{(\rm Ag)}$. We recall that $\Delta\lambda$ was chosen sufficiently large so that for separation between the mirrors equal to $\lambda/2 + \Delta\lambda$, the resonance condition breaks down. In our case $\Delta\lambda = \lambda/q$.

By analyzing Eq. (20) with account of computational results for the Casimir pressure, we find that this equality holds for $d = 1.175$ nm (which corresponds to the metallic mirror containing five atomic layers). In so doing, $\mathcal{R}^{(\rm Ag)} = 0.934$, $q = 230$, and $\Delta\lambda = 2.3$ nm. This leads to the Casimir pressure in the vertical position of the wall equal to $P = -180.4$ mPa, i.e., to the attractive Casimir force $F = PD_1^2 = -0.45$ nN and to the repulsive force of the same magnitude due to the light pressure.

At the end of this section, we briefly discuss the role of various background effects, such as electric forces due to a residual potential difference, radiation friction, and bolometric forces. For metallic mirrors used in the optical chopper, the role of residual electric force can be made negligibly small by the Ar-ion cleaning procedure developed recently in application to the Casimir-based microdevices in Ref. [72]. For the values of the light pressure considered above, the role of radiation friction and other optomechanical effects remains negligibly small [52,53].

The bolometric force arises due to light absorption. In optomechanical systems, bolometric forces may lead to a deflection of a specially optimized microlever having the spring constant of approximately 0.01 N/m [73]. Simple calculation shows that to reach a deflection of the top of our wall for 2.3 nm under the influence of the Casimir force calculated above, the spring constant of a wall, supporting the right mirror, should be equal to at least 0.1 N/m, i.e., by an order of magnitude larger. The bolometric forces may make only a negligibly small impact on an Al-coated wall with a relatively high resistance to tilting. This makes their possible role in the proposed device inessential.

Creation of the Fabry-Perot microfilter with the above parameters makes it possible to obtain discrete pulses of the transmitted light from a continuous wave of incident light. For the found value of $d = 1.175$ nm, providing the desired equality between the magnitudes of the Casimir force and the light-pressure force, one obtains the transmittance $\mathcal{T}^{(\rm Ag)} = 0.0436$, the light power entering the resonator $N_{\rm in}\mathcal{T}^{(\rm Ag)} = 0.305$ mW, and the power of the amplified light $N_{\rm res} \approx 70$ mW. The power of transmitted pulses leaving the microfilter can be determined in two ways as $N_{\rm tr} = \mathcal{T}^{(\rm Ag)}N_{\rm res}$ or as $\tau N_{\rm in}$, where, in accordance with Eq. (17), $\tau = 0.44$, leading to the common result $N_{\rm tr} \approx 3$ mW.

V. CONCLUSIONS AND DISCUSSION

In the foregoing, we propose the possibility of creating the novel microdevice driven by the vacuum fluctuations of the electromagnetic field. This device includes the Fabry-Perot microfilter with two parallel atomically thin metallic mirrors separated only slightly in excess of the half wavelength of an incident light. One of these mirrors should be deposited on the sufficiently thin wall subjected to bending under the competing impact of the attractive Casimir force and (in the presence of a continuous wave produced by the source laser) of the repulsive force due to the light pressure. As a result, the resonance condition alternatively obeys and breaks down, and the filter resonator periodically produces the pulses of transmitted light. Thus, the proposed microdevice can work as an optical chopper without using any kinds of rotating wheels usually employed in mechanically based choppers.

To demonstrate the feasibility of the proposed microdevice, we develop a theoretical description of both the Casimir force acting between atomically thin metallic mirrors deposited on dielectric substrates and of the reflectivity properties in the Fabry-Perot microfilter formed by these mirrors. It should be noted that calculation of both the Casimir force and the reflectance and transmittance of the boundary surfaces in a microfilter in the case of atomically thin mirrors is not trivial. For the Casimir force, where several first Matsubara frequencies contribute essentially at the separation considered, it is necessary to take into account an anisotropy in the dielectric properties of metallic mirrors. When calculating the reflectivity properties of an atomically thin metallic film to visible light, the use of the standard, Fresnel, reflection coefficients leads to contradictions with the measurement data, and in this case several phenomenological approaches have been developed in the literature. We use the version of the Lifshitz theory adapted for anisotropic materials to calculate the Casimir force and one of such phenomenological approaches to calculate the reflectivity properties in the Fabry-Perot microfilter. The specific values of all parameters of the proposed microdevice are determined, which ensures its workability.

In the experimental realization of the proposed setup, it is desirable to perform control measurements of the reflectance and transmittance of a unit wall made of quartz glass with deposited atomically thin metallic films of various thicknesses, as well as of its stiffness. This will help to confirm the physical nature of all acting forces and the suitability of the phenomenological approach used to calculate the reflectivity properties.

To conclude, the proposed optical chopper driven by the Casimir force may find prospective applications in the emerging area of nanotechnological devices exploiting quantum fluctuations of the electromagnetic field for their functionality.

ACKNOWLEDGMENT

The work of V.M.M. is partially supported by the Russian Government Program of Competitive Growth of Kazan Federal University.

[1] J. J. Allen, *Micro Electro Mechanical System Design* (CRC Press, New York, 2005).

[2] Y. Srivastava, A. Widom, and M. H. Friedman, Microchips as Precision Quantum-Electrodynamic Probes, Phys. Rev. Lett. **55**, 2246 (1985).

[3] Y. Srivastava and A. Widom, Quantum electrodynamic processes in electrical-engineering circuits, Phys. Rep. **148**, 1 (1987).

[4] V. A. Parsegian, *Van der Waals Forces: A Handbook for Biologists, Chemists, Engineers, and Physicists* (Cambridge University Press, Cambridge, 2005).

[5] M. Bordag, G. L. Klimchitskaya, U. Mohideen, and V. M. Mostepanenko, *Advances in the Casimir Effect* (Oxford University Press, Oxford, 2015).

[6] F. M. Serry, D. Wallicer, and G. J. Maclay, The anharmonic Casimir oscillator (ACO)—The Casimir effect in a model microelectromechanical system, J. Microelectromech. Syst. **4**, 193 (1995).

[7] G. Palasantzas, Contact angle influence on the pull-in voltage of microswitches in the presence of capillary and quantum vacuum effects, J. Appl. Phys. **101**, 053512 (2007).

[8] G. Palasantzas, Pull-in voltage of microswitch rough plates in the presence of electromagnetic and acoustic Casimir forces, J. Appl. Phys. **101**, 063548 (2007).

[9] E. Buks and M. L. Roukes, Stiction, adhesion, and the Casimir effect in micromechanical systems, Phys. Rev. B **63**, 033402 (2001).

[10] E. Buks and M. L. Roukes, Metastability and the Casimir effect in micromechanical systems, Europhys. Lett. **54**, 220 (2001).

[11] H. B. Chan, V. A. Aksyuk, R. N. Kleiman, D. J. Bishop, and F. Capasso, Quantum mechanical actuation of microelectromechanical system by the Casimir effect, Science **291**, 1941 (2001).

[12] H. B. Chan, V. A. Aksyuk, R. N. Kleiman, D. J. Bishop, and F. Capasso, Nonlinear Micromechanical Casimir Oscillator, Phys. Rev. Lett. **87**, 211801 (2001).

[13] G. L. Klimchitskaya, U. Mohideen, and V. M. Mostepanenko, The Casimir force between real materials: Experiment and theory, Rev. Mod. Phys. **81**, 1827 (2009).

[14] L. M. Woods, D. A. R. Dalvit, A. Tkatchenko, P. Rodriguez-Lopez, A. W. Rodriguez, and R. Podgornik, Materials perspective on Casimir and van der Waals interactions, Rev. Mod. Phys. **88**, 045003 (2016).

[15] R. S. Decca, E. Fischbach, G. L. Klimchitskaya, D. E. Krause, D. López, and V. M. Mostepanenko, Improved tests of extra-dimensional physics and thermal quantum field theory from new Casimir force measurements, Phys. Rev. D **68**, 116003 (2003).

[16] R. S. Decca, D. López, E. Fischbach, G. L. Klimchitskaya, D. E. Krause, and V. M. Mostepanenko, Precise comparison of theory and new experiment for the Casimir force leads to stronger constraints on thermal quantum effects and long-range interactions, Ann. Phys. (N.Y.) **318**, 37 (2005).

[17] R. S. Decca, D. López, E. Fischbach, G. L. Klimchitskaya, D. E. Krause, and V. M. Mostepanenko, Tests of new physics from precise measurements of the Casimir pressure between two gold-coated plates, Phys. Rev. D **75**, 077101 (2007).

[18] R. S. Decca, D. López, E. Fischbach, G. L. Klimchitskaya, D. E. Krause, and V. M. Mostepanenko, Novel constraints on light elementary particles and extra-dimensional physics from the Casimir effect, Eur. Phys. J. C **51**, 963 (2007).

[19] C.-C. Chang, A. A. Banishev, R. Castillo-Garza, G. L. Klimchitskaya, V. M. Mostepanenko, and U. Mohideen, Gradient of the Casimir force between Au surfaces of a sphere and a plate measured using an atomic force microscope in a frequency-shift technique, Phys. Rev. B **85**, 165443 (2012).

[20] A. A. Banishev, C.-C. Chang, G. L. Klimchitskaya, V. M. Mostepanenko, and U. Mohideen, Measurement of the gradient of the Casimir force between a nonmagnetic gold sphere and a magnetic nickel plate, Phys. Rev. B **85**, 195422 (2012).

[21] A. A. Banishev, G. L. Klimchitskaya, V. M. Mostepanenko, and U. Mohideen, Demonstration of the Casimir Force Between Ferromagnetic Surfaces of a Ni-Coated Sphere and a Ni-Coated Plate, Phys. Rev. Lett. **110**, 137401 (2013).

[22] A. A. Banishev, G. L. Klimchitskaya, V. M. Mostepanenko, and U. Mohideen, Casimir interaction between two magnetic metals in comparison with nonmagnetic test bodies, Phys. Rev. B **88**, 155410 (2013).

[23] G. Bimonte, D. López, and R. S. Decca, Isoelectronic determination of the thermal Casimir force, Phys. Rev. B **93**, 184434 (2016).

[24] F. Chen, U. Mohideen, G. L. Klimchitskaya, and V. M. Mostepanenko, Investigation of the Casimir force between metal and semiconductor test bodies, Phys. Rev. A **72**, 020101(R) (2005).

[25] F. Chen, G. L. Klimchitskaya, V. M. Mostepanenko, and U. Mohideen, Demonstration of the Difference in the Casimir Force for Samples with Different Charge-Carrier Densities, Phys. Rev. Lett. **97**, 170402 (2006).

[26] F. Chen, U. Mohideen, G. L. Klimchitskaya, and V. M. Mostepanenko, Experimental test for the conductivity properties from the Casimir force between metal and semiconductor, Phys. Rev. A **74**, 022103 (2006).

[27] F. Chen, G. L. Klimchitskaya, V. M. Mostepanenko, and U. Mohideen, Demonstration of optically modulated dispersion forces, Opt. Express **15**, 4823 (2007).

[28] F. Chen, G. L. Klimchitskaya, V. M. Mostepanenko, and U. Mohideen, Control of the Casimir force by the modification of dielectric properties with light, Phys. Rev. B **76**, 035338 (2007).

[29] G. Torricelli, P. J. van Zwol, O. Shpak, C. Binns, G. Palasantzas, B. J. Kooi, V. B. Svetovoy, and M. Wuttig, Switching Casimir force with phase-change materials, Phys. Rev. A **82**, 010101(R) (2010).

[30] S. de Man, K. Heeck, R. J. Wijngaarden, and D. Iannuzzi, Halving the Casimir Force with Conductive Oxides, Phys. Rev. Lett. **103**, 040402 (2009).

[31] S. de Man, K. Heeck, and D. Iannuzzi, Halving the Casimir force with conductive oxides: Experimental details, Phys. Rev. A **82**, 062512 (2010).

[32] C.-C. Chang, A. A. Banishev, G. L. Klimchitskaya, V. M. Mostepanenko, and U. Mohideen, Reduction of the Casimir Force from Indium Tin Oxide Film by UV Treatment, Phys. Rev. Lett. **107**, 090403 (2011).

[33] A. A. Banishev, C.-C. Chang, R. Castillo-Garza, G. L. Klimchitskaya, V. M. Mostepanenko, and U. Mohideen, Modifying the Casimir force between indium tin oxide plate and Au sphere, Phys. Rev. B **85**, 045436 (2012).

[34] M. Sedighi, V. B. Svetovoy, and G. Palasantzas, Casimir force measurements from carbide surfaces, Phys. Rev. B **93**, 085434 (2016).

[35] H. B. Chan, Y. Bao, J. Zou, R. A. Cirelli, F. Klemens, W. M. Mansfield, and C. S. Pai, Measurement of the Casimir Force Between a Gold Sphere and a Silicon Surface with Nanoscale Trench Arrays, Phys. Rev. Lett. **101**, 030401 (2008).

[36] Y. Bao, R. Guérout, J. Lussange, A. Lambrecht, R. A. Cirelli, F. Klemens, W. M. Mansfield, C. S. Pai, and H. B. Chan, Casimir Force on a Surface with Shallow Nanoscale Corrugations: Geometry and Finite Conductivity Effects, Phys. Rev. Lett. **105**, 250402 (2010).

[37] H.-C. Chiu, G. L. Klimchitskaya, V. N. Marachevsky, V. M. Mostepanenko, and U. Mohideen, Demonstration of the asymmetric lateral Casimir force between corrugated surfaces in nonadditive regime, Phys. Rev. B **80**, 121402(R) (2009).

[38] H.-C. Chiu, G. L. Klimchitskaya, V. N. Marachevsky, V. M. Mostepanenko, and U. Mohideen, Lateral Casimir force between sinusoidally corrugated surfaces: Asymmetric profiles, deviations from the proximity force approximation, and comparison with exact theory, Phys. Rev. B **81**, 115417 (2010).

[39] F. Intravaia, S. Koev, I. W. Jung, A. A. Talin, P. S. Davids, R. S. Decca, V. A. Aksyuk, D. A. R. Dalvit, and D. López, Strong Casimir force reduction through metallic surface nanostructuring, Nat. Commun. **4**, 2515 (2013).

[40] J. Barcenas, L. Reyes, and R. Esquivel-Sirvent, Scaling of micro- and nanodevices actuated by the Casimir force, Appl. Phys. Lett. **87**, 263106 (2005).

[41] R. Esquivel-Sirvent and R. Pérez-Pascual, Geometry and charge carrier induced stability in Casimir actuated nanodevices, Eur. Phys. J. B **86**, 467 (2013).

[42] W. Broer, G. Palasantzas, J. Knoester, and V. B. Svetovoy, Significance of the Casimir force and surface roughness for actuation dynamics of MEMS, Phys. Rev. B **87**, 125413 (2013).

[43] M. Sedighi, W. Broer, G. Palasantzas, and B. J. Kooi, Sensitivity of micromechanical actuation on amorphous to crystalline phase transformations under the influence of Casimir forces, Phys. Rev. B **88**, 165423 (2013).

[44] W. Broer, H. Waalkens, V. B. Svetovoy, J. Knoester, and G. Palasantzas, Nonlinear Actuation Dynamics of Driven Casimir Oscillators with Rough Surfaces, Phys. Rev. Appl. **4**, 054016 (2015).

[45] J. Zou, Z. Marcet, A. W. Rodriguez, M. T. H. Reid, A. P. McCauley, I. I. Kravchenko, T. Lu, Y. Bao, S. G. Johnson, and H. B. Chan, Casimir forces on a silicon micromechanical chip, Nat. Commun. **4**, 1845 (2013).

[46] L. Tang, M. Wang, C. Y. Ng, M. Nicolic, C. T. Chan, A. W. Rodriguez, and H. B. Chan, Measurement of non-monotonic Casimir forces between silicon nanostructures, Nat. Photonics **11**, 97 (2017).

[47] N. Inui, Optical switching of a graphene mechanical switch using the Casimir effect, J. Appl. Phys. **122**, 104501 (2017).

[48] X.-F. Liu, Y. Li, and H. Jing, Casimir switch: Steering optical transparancy with vacuum forces, Sci. Rep. **6**, 27102 (2016).

[49] G. L. Klimchitskaya, U. Mohideen, and V. M. Mostepanenko, Casimir and van der Waals force between two plates or a sphere (lens) above a plate made of real metals, Phys. Rev. A **61**, 062107 (2000).

[50] V. M. Petrov, M. P. Petrov, V. V. Bryksin, J. Petter, and T. Tschudi, Optical detection of the Casimir force between macroscopic objects, Opt. Lett. **32**, 3167 (2006).

[51] V. M. Petrov, M. P. Petrov, V. V. Bryksin, J. Petter, and T. Tschudi, Casimir force measurement using dynamic holography, JETP **104**, 696 (2007) [Zh. Eksp. Teor. Fiz. **131**, 798 (2007)].

[52] M. Aspelmeyer, T. J. Kippenberg, and F. Marquardt, *Cavity Optomechanics* (Springer, Berlin, 2014).

[53] M. Aspelmeyer, T. J. Kippenberg, and F. Marquardt, Cavity optomechanics, Rev. Mod. Phys. **86**, 1391 (2014).

[54] M. Boström, C. Persson, and Bo E. Sernelius, Casimir force between atomically thin gold films, Eur. Phys. J. B **86**, 43 (2013).

[55] D. S. Ghosh, *Ultrathin Metal Transparent Electrodes for the Optoelectronics Industry* (Springer, Cham, 2013).

[56] V. Petrov, J. Hahn, J. Petter, M. Petrov, and T. Tschudi, Precise subnanometer control of the position of a macro object by light pressure, Opt. Lett. **30**, 3138 (2005).

[57] O. Suchoi and E. Buks, Sensing dispersive and dissipative forces by an optomechanical cavity, Europhys. Lett. **115**, 14001 (2016).

[58] M. S. Tomaš, Casimir force in absorbing multilayers, Phys. Rev. A **66**, 052103 (2002).

[59] C. Raabe, L. Knöll, and D.-G. Welsch, Three-dimensional Casimir force between absorbing multilayer dielectrics, Phys. Rev. A **68**, 033810 (2003).

[60] G. L. Klimchitskaya and V. M. Mostepanenko, Casimir and van der Waals energy of anisotropic atomically thin metallic films, Phys. Rev. B **92**, 205410 (2015).

[61] V. M. Mostepanenko, Special features of the thermal Casimir effect across a uniaxial anisotropic film, Phys. Rev. A **92**, 012511 (2015).

[62] L. Bergström, Hamaker constants of inorganic materials, Adv. Colloid Interface Sci. **70**, 125 (1997).

[63] *Handbook of Optical Constants of Solids*, edited by E. D. Palik (Academic, New York, 1985).

[64] C. Kittel, *Introduction to Solid State Physics* (Wiley, New York, 1996).

[65] L. D. Landau, E. M. Lifshitz, and L. P. Pitaevskii, *Electrodynamics of Continuous Media* (Pergamon, Oxford, 1984).

[66] D. J. Nash and J. R. Sambles, Surface plasmon study of the optical dielectric function of silver, J. Mod. Opt. **43**, 81 (1996).

[67] I. R. Hooper and J. R. Sambles, Some considerations on the transmissivity of thin metal films, Opt. Express **16**, 17258 (2008).

[68] T. A. Kudykina, Boundary conditions in case of electromagnetic wave absorption, Phys. Status Solidi (b) **160**, 365 (1990).

[69] T. A. Kudykina, Dispersion and propagation of light in crystals in the exciton absorption region, Phys. Status Solidi (b) **165**, 591 (1991).

[70] S. A. Kovalenko, Optical properties of thin metal films, Semicond. Phys. Quantum Electron. Optoelectron. **2**, 13 (1999).

[71] M. Born and E. Wolf, *Principles of Optics* (Cambridge University Press, Cambridge, 1999).

[72] J. Xu, G. L. Klimchitskaya, V. M. Mostepanenko, and U. Mohideen, Reducing detrimental electrostatic effects in Casimir-force measurements and Casimir-force-based microdevices, Phys. Rev. A **97**, 032501 (2018).

[73] C. Metzger, M. Ludwig, C. Neuenhahn, A. Ortlieb, I. Favero, K. Karrai, and F. Marquardt, Self-Induced Oscillations in an Optomechanical System Driven by Bolometric Backreaction, Phys. Rev. Lett. **101**, 133903 (2008).